

Replacing Alkyl with Oligo(ethylene glycol) as Side Chains of Conjugated Polymers for Close π – π Stacking

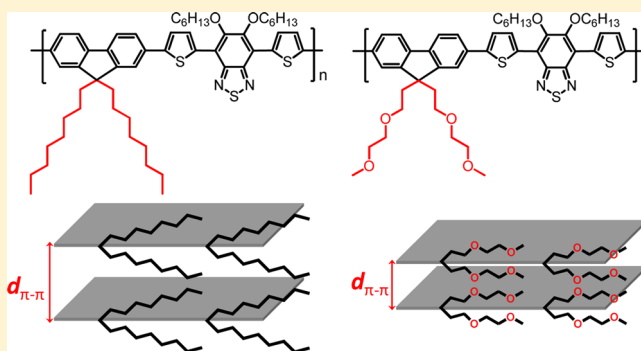
Bin Meng,^{†,‡} Haiyang Song,[†] Xingxing Chen,^{†,‡} Zhiyuan Xie,[†] Jun Liu,^{*,†} and Lixiang Wang^{*,†}

[†]State Key Laboratory of Polymer Physics and Chemistry, Changchun Institute of Applied Chemistry, Chinese Academy of Sciences, Changchun 130022, P. R. China

[‡]University of Chinese Academy of Sciences, Beijing 100039, P. R. China

Supporting Information

ABSTRACT: We synthesize and systematically study a series of conjugated polymers with oligo(ethylene glycol) (OEG) or alkyl chain as the side chain and poly[2,7-fluorene-*alt*-5,5'-(4,7-di-2-thienyl-2,1,3-benzothiadiazole)] as the polymer backbone. Replacing alkyl chain with OEG chain can decrease the π – π stacking distance of polymer backbone in thin film from 0.44 to 0.41 nm because OEG chain is more flexible than alkyl chain. As the result, the conjugated polymer with OEG side chain exhibits higher hole mobility, red-shifted absorption spectrum in thin film and smaller bandgap than those of the conjugated polymer with alkyl side chain. With the increase of the length of OEG side chain, the resulting conjugated polymers exhibit unchanged π – π stacking distance and decreased hole mobility. Moreover, owing to the large polarity of OEG chain, OEG side chain makes the conjugated polymer suitable for polymer solar cell (PSC) devices processed with polar nonhalogenated solvent, methoxybenzene. A power conversion efficiency of 4.04% is demonstrated with the resulting PSC devices. This work provides the new insight into the effect of OEG side chain on conjugated polymer, which can be used in the molecular design of novel conjugated polymer materials with excellent optoelectronic device performance.

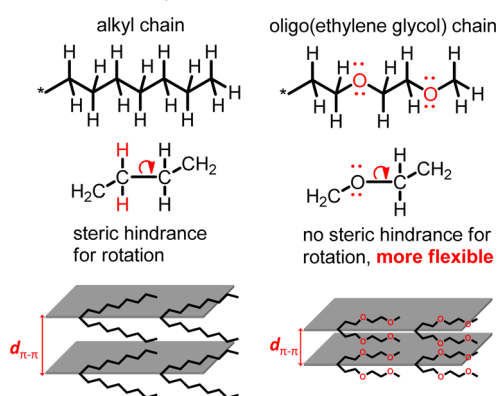


INTRODUCTION

Conjugated polymers have been widely used in optoelectronic devices, such as organic light-emitting diodes (OLEDs), organic field-effect transistors (OFETs), and polymer solar cells (PSCs), with the great advantages of low cost, flexibility, and solution processing.¹ For solubility of conjugated polymers, a rigid conjugated polymer backbone is always equipped with an alkyl side chain.² Oligo(ethylene glycol) (OEG) chain is well-known for its hydrophilicity and is always used to endow molecules/polymers solubility in water or polar organic solvents.³ Thus, OEG chain has been used as side chain of conjugated polymers for efficient OLED, OFET, and PSC devices processed with polar nonhalogenated solvents.⁴ As optoelectronic properties of conjugated polymers are affected by the side chain,⁵ the effect of OEG side chain on properties of conjugated polymers is less investigated and poorly understood. Researchers may doubt whether hydrophilic OEG side chain would disturb the π – π stacking of hydrophobic polymer backbone in conjugated polymers. This manuscript aims to provide an insight into the effect of OEG side chain on conjugated polymers.

We note that OEG chain is more flexible than alkyl chain. As shown in Scheme 1, the two hydrogen atom in CH_2 unit act as steric hindrance for the rotation of CH_2 – CH_2 unit in alkyl chain, while the two lone electron pair in oxygen atom result in no steric hindrance for the rotation of O – CH_2 in OEG chain.⁶ Therefore,

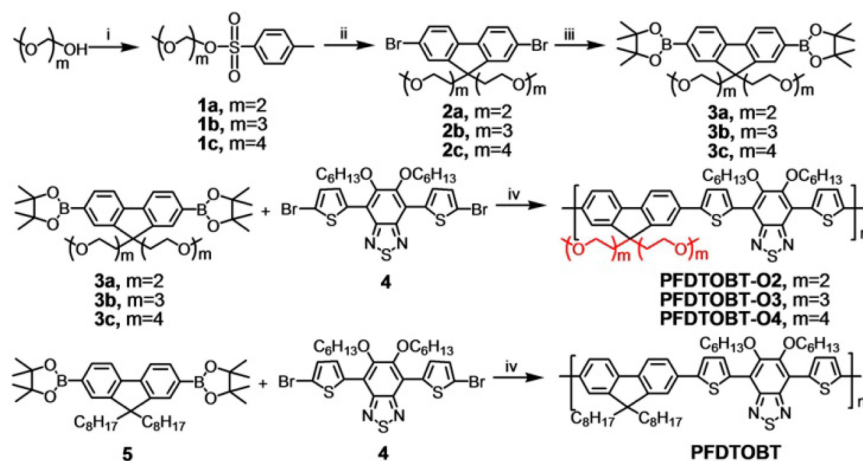
Scheme 1. Schematic Illustration of the Superior Flexibility of OEG Chain Than Alkyl Chain



the energy barrier of the rotation of O – CH_2 in OEG chain ($E = 0.08$ eV) is smaller than that of CH_2 – CH_2 in alkyl chain ($E = 0.11$ eV),⁶ making OEG chain more flexible than alkyl chain. For conjugated polymers, alkyl side chain impedes the close π – π

Received: April 5, 2015

Revised: June 10, 2015

Scheme 2. Chemical Structures and Synthetic Routes of the Four Polymers^a

^aReagents and conditions: (i) *p*-tolylsulfate chloride, NaOH (aq), THF, room temperature; (ii) 2,7-dibromo-fluorene, NaOH (aq, 50 wt %), (*n*-C₄H₉)₄NBr, toluene, reflux; (iii) 4,4,5,5-tetramethyl-2-(4,4,5,5-tetramethyl-1,3,2-dioxaborolan-2-yl)-1,3,2-dioxaborolane, Pd(dppf)Cl₂, CH₃COOK, DMF, 90 °C; (iv) Pd(PPh₃)₄, K₂CO₃ (aq, 2 M), Aliquat 336, toluene, 100 °C.

Table 1. Molecular Weights, Thermal Properties, π - π Stacking Distance, and Hole Mobility of the Four Polymers

polymer	M_n	PDI	T_d (°C)	T_{cc} (°C)	T_m (°C)	$d_{\pi-\pi}$ (nm)	μ_h (cm ² V ⁻¹ s ⁻¹)
PFDTOBT	59600	2.86	310	—	—	0.44	1.48×10^{-6}
PFDTOBT-O2	55000	2.30	315	118	220	0.41	1.10×10^{-5}
PFDTOBT-O3	78760	2.99	320	123	148	0.41	2.61×10^{-6}
PFDTOBT-O4	50100	2.04	322	—	—	0.41	5.07×10^{-7}

stacking of polymer backbone because the stacking distance of alkyl chain (4.1 Å) is larger than that of ideal π - π stacking distance (ca. 3.4 Å).⁷ Therefore, compared with alkyl side chain, the more flexible OEG side chain can favor the π - π stacking of polymer backbone of conjugated polymers. As optical and electronic properties of conjugated polymers are affected by the solid state organization of polymer backbone,⁸ the close π - π stacking favored by OEG side chain can affect the optical and electronic properties of conjugated polymers.

Motivated by the above data and analysis, in order to disclose the effect of OEG side chain on conjugated polymer, we synthesize and systematically study a series of conjugated polymers with OEG of different length or alkyl chain as the side chain and poly[2,7-fluorene-*alt*-5,5-(4,7-di-2-thienyl-2,1,3-benzothiadiazole)] (PFDTOBT-*m*) as the conjugated polymer backbone. We find that replacing alkyl chain with OEG chain can decrease the π - π stacking distance of polymer backbone from 0.44 to 0.41 nm. As the result, the polymers with OEG side chain have higher hole mobility and smaller bandgap than those of the polymer with alkyl side chain. Moreover, owing to the large polarity of OEG chain, OEG side chain makes the conjugated polymer suitable for PSC devices processed with polar nonhalogenated solvent. This work provides the new insight into the effect of OEG side chain on conjugated polymer, which can be used in the molecular design of novel conjugated polymer materials with excellent optoelectronic device performance.

RESULTS AND DISCUSSION

Molecular Design. Scheme 2 shows the chemical structures of the four conjugated polymers with the same polymer backbone and different side chains. PFDTOBT-*m* is selected as the conjugated polymer backbone⁹ because each fluorene unit can be functionalized with two side chains with “sticking-out”

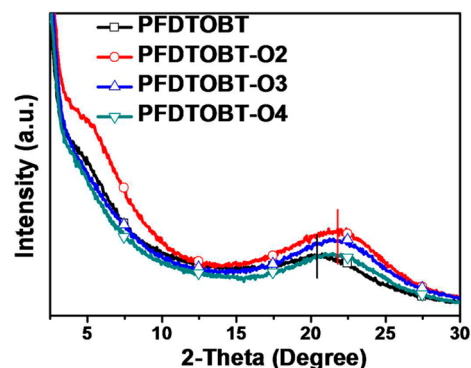


Figure 1. GI-XRD patterns of the four polymers.

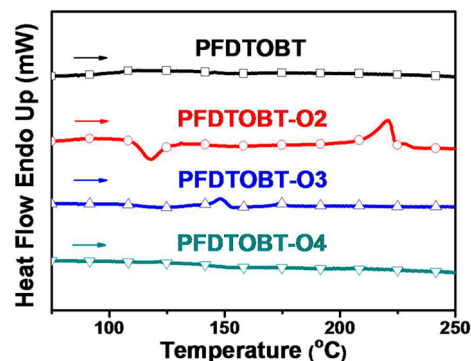


Figure 2. DSC second heating curves of the four polymers.

configuration. Since the “sticking-out” side chains can prevent the close stacking of the conjugated polymer backbone, the flexibility of the side chains may obviously affect the π - π stacking distance of the polymer backbone.¹⁰ Thus, PFDTOBT-*m* is very

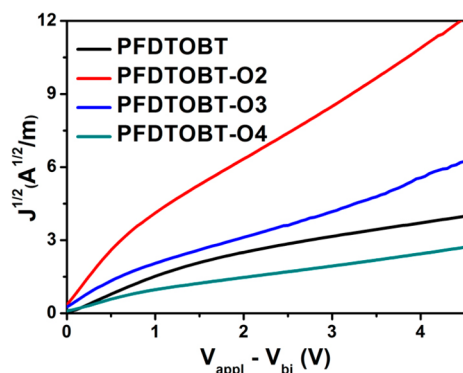


Figure 3. $J^{1/2}$ vs $(V_{\text{appl}} - V_{\text{bi}})$ curves of the hole-only devices of the four polymers. (device structure: ITO/PEDOT:PSS/polymer/Au).

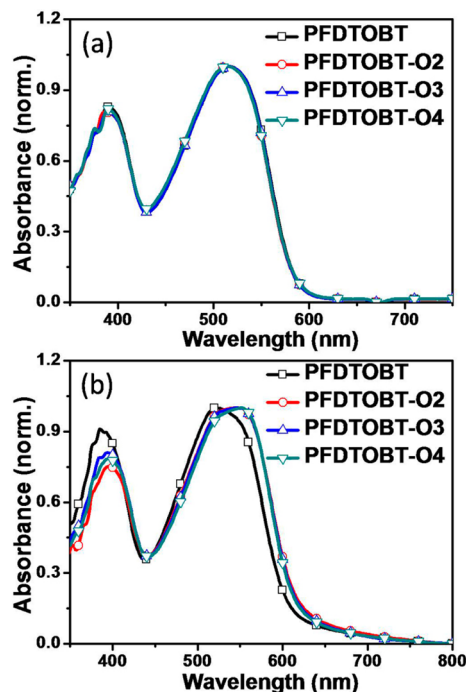


Figure 4. UV-vis absorption spectra of the four polymers in CB solution (a) and in thin film (b).

suitable for investigation of the effect of side chains on π - π stacking of polymer backbone. To ensure good solubility and high molecular weight of all the polymers, we use two hexyl unit on the 2,1,3-benzothiadiazole unit.¹¹ As shown in Scheme 2, PFDTOBT with nonpolar octyl chains on the fluorene unit is a conventional conjugated polymer and is used here as the reference.¹² To investigate the effect of OEG side chain, we devise PFDTOBT-O2 with di(ethylene glycol) side chains of similar length with that of the octyl chains in PFDTOBT. To

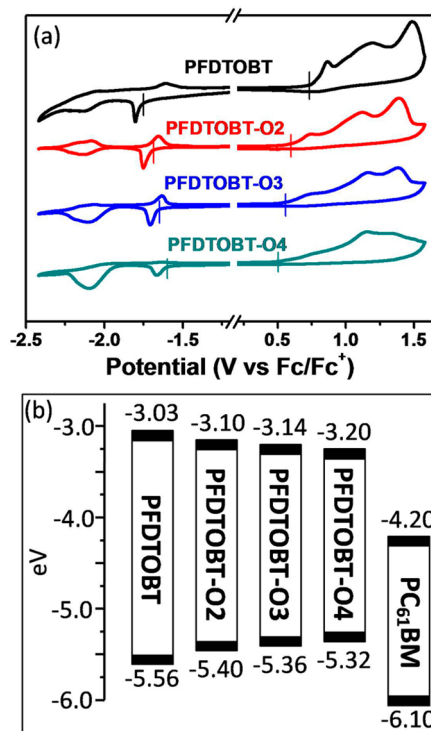


Figure 5. (a) Cyclic voltammogram of the four polymers in thin film. (b) HOMO and LUMO energy levels of the four polymers and PC₆₁BM.

further study the effect of the length of OEG side chain, we design PFDTOBT-O3 and PFDTOBT-O4 with tri(ethylene glycol) side chain and tetra(ethylene glycol) side chain, respectively.

Synthesis. The synthetic routes for the four polymers are depicted in Scheme 2. Tosylation of corresponding hydroxyl compound and subsequent alkylation with 2,7-dibromofluorene readily gave 2a–c. The key monomers 3a–c was prepared by Miyaura borylation reaction of 2a–c and bis(pinacolato)-diboron. Finally, we synthesized the four polymers using Pd(0)-catalyzed Suzuki polycondensation with the corresponding diboronic ester monomer and the dibromo monomer. All these polymers exhibit good solubility in common chlorinated solvents, e.g. chloroform, CB, and in some nonhalogenated solvents, e.g., xylene, methoxybenzene (MOB). The chemical structures of the polymers are confirmed by ¹H NMR and elemental analysis. Their molecular weights are estimated by gel permeation chromatography (GPC) using tetrahydrofuran (THF) as the eluent and monodisperse polystyrene as the standards. As listed in Table 1, the four polymers all have number-average molecular weight (M_n) higher than 50 000 and polydispersities (PDI) around 2.5.

Stacking in the Solid State. To investigate the solid state organization of polymer chains, grazing incidence X-ray

Table 2. Photophysical and Electrochemical Properties of the Polymers

polymer	$\lambda_{\text{max}}^{\text{sol}}$ (nm)	ξ ($\times 10^4$ L·mol ⁻¹ ·cm ⁻¹)	$\lambda_{\text{max}}^{\text{film}}$ (nm)	$\lambda_{\text{onset}}^{\text{film}}$ (nm)	E_g^{opt} (eV)	$E_{\text{onset}}^{\text{ox}}$ (V) ^a	$E_{\text{onset}}^{\text{red}}$ (V) ^a	HOMO (eV)	LUMO (eV)	E_g^{ec} (eV)
PFDTOBT	517	5.64	523	606	2.05	0.76	-1.77	-5.56	-3.03	2.53
PFDTOBT-O2	515	5.25	547	616	2.01	0.60	-1.70	-5.40	-3.10	2.30
PFDTOBT-O3	517	5.39	547	615	2.02	0.56	-1.66	-5.36	-3.14	2.22
PFDTOBT-O4	515	4.68	549	613	2.02	0.52	-1.60	-5.32	-3.20	2.12

^aOnset potential vs Fc/Fc⁺.

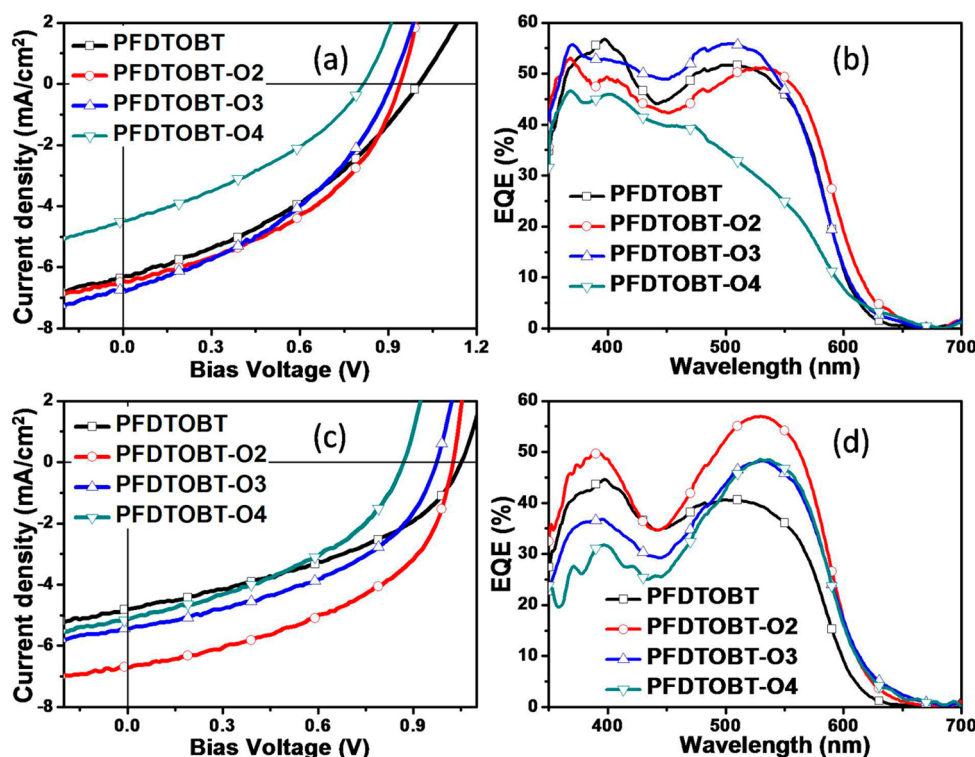


Figure 6. J - V curves (a) and EQE curves (b) of the PSC devices based on the polymers processed with CB as the solvent. J - V curves (c) and EQE curves (d) of the PSC devices based on the polymers processed with MOB as the solvent.

diffraction (GI-XRD) of spin-coated film of the four polymers was performed. As shown in Figure 1, all the four polymers show weak diffraction peaks due to the lamellar stacking and moderate diffraction peaks assigned to the π - π stacking of the polymer backbone. The diffraction peak of PFDTOBT with alkyl side chain is at $2\theta = 20.3^\circ$, corresponding to the π - π stacking distance ($d_{\pi-\pi}$) of 0.44 nm (Table 1).¹⁰ In comparison, all the three polymers having OEG side chains show $2\theta = 21.7^\circ$, corresponding to the $d_{\pi-\pi}$ of 0.41 nm (Table 1). Compared with alkyl side chain, OEG side chain favors more compact π - π stacking of the conjugated polymer backbone because OEG side chain is more flexible with smaller steric hindrance for the π - π stacking. Researchers always doubt whether the hydrophilicity of OEG side chain disturbs π - π stacking of hydrophobic conjugated polymer backbone. Comparison of the XRD patterns of PFDTOBT-O2 and PFDTOBT unambiguously verifies that OEG side chain favors ordered organization of polymer backbone in solid state and that the hydrophilicity of OEG side chain cannot play a dominant role. Moreover, the same $d_{\pi-\pi}$ of PFDTOBT-O2, PFDTOBT-O3, and PFDTOBT-O4 suggests that the length of OEG side chain does not affect the π - π stacking distance of conjugated polymer backbone. Because optical and electronic properties of conjugated polymers are affected by organization of polymer chains in solid state, the close π - π stacking with OEG side chains is expected to change the properties of the polymers in thin film.

Thermal Properties. According to thermogravimetric analysis (TGA), all the four polymers have good thermal stability with thermal degradation temperature (T_d) higher than 310°C (Table 1). Then differential scanning calorimetry (DSC) was employed to investigate the thermodynamic behaviors of the four polymers. The second heating curves of these polymers are shown in Figure 2. There is no obvious exothermal and endothermal peak for PFDTOBT in the temperature range 50–

250°C . In contrast, the DSC curve of PFDTOBT-O2 shows an exothermal peak at 118°C with an area of $6.93\text{ J}\cdot\text{g}^{-1}$ and an endothermal peak at 220°C with an area of $11.77\text{ J}\cdot\text{g}^{-1}$, which is attributed to the cold crystallization and melting of PFDTOBT-O2, respectively. The comparison of the DSC curves of PFDTOBT and PFDTOBT-O2 suggests that OEG side chain makes the resulting polymer more crystalline in solid state. This is consistent with the closer π - π stacking of conjugated polymer backbone of PFDTOBT-O2 than that of PFDTOBT. The cold crystallization peak ($T_{cc} = 123^\circ\text{C}$, $1.71\text{ J}\cdot\text{g}^{-1}$) and melting peak ($T_m = 148^\circ\text{C}$, $1.62\text{ J}\cdot\text{g}^{-1}$) in DSC curves become weak for PFDTOBT-O3. The two peaks even diminish for PFDTOBT-O4, indicating that longer OEG side chain makes the resulting polymer less crystalline.

Hole Mobility. The hole mobility of the polymers was estimated using space charge limited current (SCLC) method according to the current density^{1/2} – voltage ($J^{1/2}$ – V) curves of the hole-only devices (device structure: ITO (indium tin oxide)/PEDOT:PSS (poly(3,4-ethylenedioxythiophene) doped with poly(styrenesulfonate))/polymer/Au) (Figure 3). As listed in Table 1, the hole mobility of PFDTOBT-O2 ($\mu_h = 1.10 \times 10^{-5}\text{ cm}^2\text{ V}^{-1}\text{ s}^{-1}$) is much higher than that of PFDTOBT ($\mu_h = 1.48 \times 10^{-6}\text{ cm}^2\text{ V}^{-1}\text{ s}^{-1}$), which is attributed to the aforementioned close π - π stacking of PFDTOBT-O2 with OEG side chain. Comparison of the hole mobility of PFDTOBT-O2, PFDTOBT-O3 and PFDTOBT-O4 implies that the hole mobility decreases with the increase of the OEG side chain length. Since side chains are inert and charge carriers transport on conjugated polymer backbone, the decreased hole mobility with increased OEG side chain length is attributed to the increased content of inert component and decreased content of conjugated polymer backbone in the polymers. The hole mobility data are consistent with the less ordered solid state

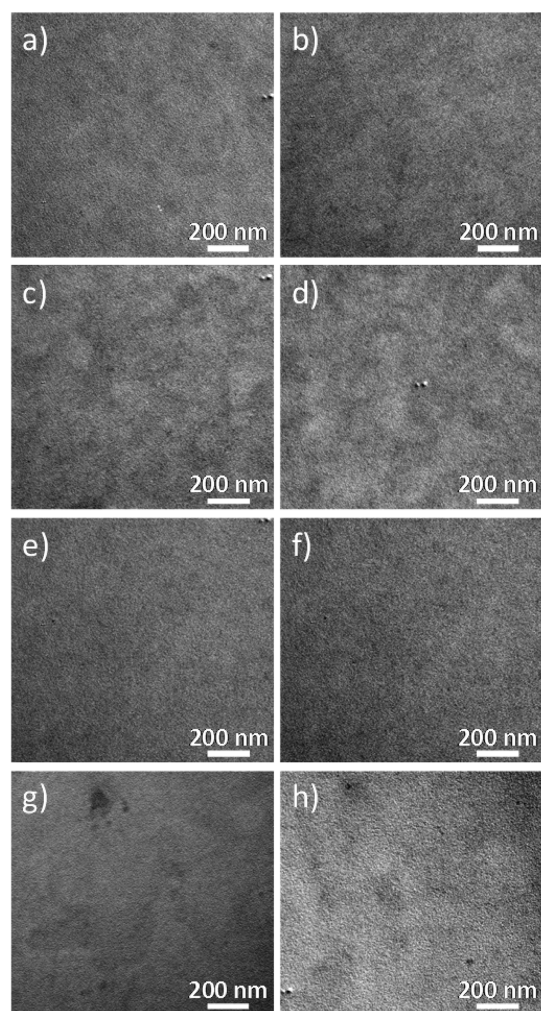


Figure 7. TEM images of the film of PFDTOBT (a, b), PFDTOBT-O2 (c, d), PFDTOBT-O3 (e, f), and PFDTOBT-O4 (g, h) blended with PC₆₁BM processed with CB (a, c, e, g) and MOB (b, d, f, h).

organization of polymer chains with increasing OEG side chain length as revealed in DSC curves and XRD patterns.

Absorption Spectra. Figure 4 shows the UV–vis absorption spectra in CB solution and in film of the four polymers. In CB solution, the four polymers exhibit identical absorption spectra with two absorption peaks at 390 and 516 nm, which are ascribed to the π – π^* transition and the intramolecular charge transfer of the polymer backbone, respectively.¹² The same absorption spectra of the four polymers with different side chains in solution imply that the OEG side chains do not affect the electronic structure of the conjugated polymer backbone in isolated state. In thin film, the long-wavelength absorption peak of PFDTOBT, PFDTOBT-O2, PFDTOBT-O3, and PFDTOBT-O4 is redshifted to 523, 547, 547, and 549 nm, respectively. The redshift of the absorption peak from in solution to in film is due to the interaction of conjugated polymer backbone in solid state.¹³ The absorption peak redshift of the three polymers with OEG side chains ($\Delta\lambda = 31$ – 33 nm) is much larger than that ($\Delta\lambda = 7$ nm) of PFDTOBT with alkyl side chain. This indicates the stronger interaction of conjugated polymer backbone owing to the smaller π – π stacking distance of the three polymers with OEG side chains compared to PFDTOBT with alkyl side chain. On the basis of the onset wavelength of absorption spectra, the optical bandgap (E_g^{opt}) of PFDTOBT is estimated to be 2.05 eV and the

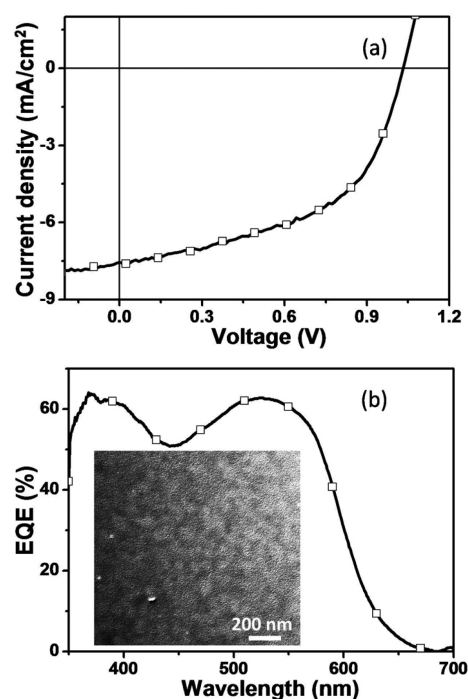


Figure 8. J – V curves (a) and EQE curves (b) of the PSC devices based on PFDTOBT-O2 processed with MOB and 5 vol % DIO. The inset is the TEM image of the film of PFDTOBT-O2:PC₆₁BM processed with MOB and 5 vol % DIO.

E_g^{opt} of PFDTOBT-O2, PFDTOBT-O3, and PFDTOBT-O4 is 2.01 eV (Table 2).

Electrochemical Properties. Cyclic voltammetry (CV) of the thin film was carried out to investigate the electrochemical properties and estimate the LUMO/HOMO energy levels of the four polymers. As shown in Figure 5a, all four polymers show both oxidation and reduction waves assigned to the conjugated polymer backbone. According to the onset potential of the oxidation waves and the reduction waves, we estimate the HOMO and LUMO energy levels of the four polymers. The results are listed in Table 2 and compared in Figure 5b. Compared with PFDTOBT, PFDTOBT-O2 with an OEG side chain of similar length shows a much decreased LUMO level and an increased HOMO level with smaller bandgap. Considering their XRD and UV/vis absorption spectra, we attribute the change of LUMO/HOMO mainly to the enhanced coplanarity of the polymer backbone in PFDTOBT-O2 because of the compact π – π stacking with flexible OEG side chain. Similar energy level change with varied π – π stacking distance been reported previously in conjugated polymers with different alkyl chains.⁵ For PFDTOBT-O2, PFDTOBT-O3, and PFDTOBT-O4, with the increase of the OEG side chain length, the HOMO level increases and the LUMO level decreases, leading to smaller bandgap. This is inconsistency with their similar absorption spectra in thin film. The reason for the inconsistency is under further investigation. As shown in Figure 5b, despite of the difference, the LUMO levels of all the four polymers are all high enough to ensure electron transfer to the typical electron acceptor, phenyl-C61-butyric acid methyl ester (PC₆₁BM), indicating that all these four polymer can be used as effective donor polymers for PSCs.¹⁴ On the other hand, the different HOMO levels of the four polymers are expected to influence the open-circuit voltage (V_{OC}) of the resulting PSC devices.¹⁴

Table 3. Characteristics of the PSC Devices of the Polymers with CB or MOB as the Processing Solvent

polymer	processing solvent	V_{OC}^a (V)	J_{SC}^a (mA/cm ²)	FF ^a	PCE ^a (%)
PFDTOBT	CB	0.99 ± 0.01	6.20 ± 0.11	0.36 ± 0.01	2.28 ± 0.07
PFDTOBT-O2	CB	0.94 ± 0.01	6.40 ± 0.06	0.42 ± 0.01	2.58 ± 0.04
PFDTOBT-O3	CB	0.90 ± 0.01	6.61 ± 0.10	0.40 ± 0.01	2.35 ± 0.07
PFDTOBT-O4	CB	0.82 ± 0.02	4.40 ± 0.09	0.34 ± 0.02	1.20 ± 0.10
PFDTOBT	MOB	1.04 ± 0.01	4.69 ± 0.11	0.41 ± 0.01	2.00 ± 0.05
PFDTOBT-O2	MOB	1.03 ± 0.01	6.79 ± 0.05	0.47 ± 0.01	3.29 ± 0.03
PFDTOBT-O3	MOB	0.96 ± 0.01	5.36 ± 0.09	0.45 ± 0.02	2.30 ± 0.05
PFDTOBT-O4	MOB	0.87 ± 0.02	5.02 ± 0.12	0.40 ± 0.01	1.72 ± 0.11
PFDTOBT-O2	MOB + DIO	1.02 ± 0.01	7.48 ± 0.06	0.52 ± 0.01	4.00 ± 0.04

^aThe data shown are the average values obtained from 6 devices with standard deviation.

PSC Devices. To evaluate and compare the photovoltaic properties of the four polymers, PSC devices were fabricated using the structure of ITO/PEDOT:PSS/polymer:PC₆₁BM/LiF/Al. The polymer:PC₆₁BM ratio was fixed to be 1:4. Both halogenated solvent CB and nonhalogenated solvent MOB were used for the spin-coating of the active layers for comparison.¹⁵ Parts a and c of Figure 6 show the J - V curves of the PSC devices of the four polymers processed with CB and MOB, respectively. The control device of PFDTOBT processed with CB exhibits a PCE of 2.35% with $V_{OC} = 1.00$ V, $J_{SC} = 6.31$ mA/cm², and FF = 0.37. In comparison, the PSC device based on PFDTOBT-O2 processed with CB shows a higher PCE of 2.62% with an obviously increased J_{SC} and FF, which may attribute to its higher hole mobility and better active layer morphology (vide infra). The comparison of the two devices suggests that OEG side chain has no negative effect on photovoltaic performance of the polymers.

It is found that PFDTOBT-O2, PFDTOBT-O3, and PFDTOBT-O4 with OEG side chains exhibit V_{OC} lower than that of PFDTOBT with alkyl side chains. Increase of the OEG side chain length leads to decrease of V_{OC} . The relationship of the V_{OC} with the chemical structure of the four polymers is consistent with the CV results and their HOMO levels (Figure 5b).¹⁴ The device of PFDTOBT with MOB as the processing solvent exhibits inferior photovoltaic performance compared with the counterpart with CB as the solvent. In contrast, the devices of PFDTOBT-O2 and PFDTOBT-O4 processed with MOB show superior photovoltaic performance than the corresponding devices processed with CB. These results suggest that OEG side chains make conjugated polymers suitable for processing with nonhalogenated solvent MOB. Among all these device, the device of PFDTOBT-O2 processed with MOB exhibits the best photovoltaic performance with the V_{OC} of 1.03 V, J_{SC} of 6.84 mA/cm², and FF of 0.47, corresponding to the PCE of 3.32%. The external quantum efficiency (EQE) curves of the devices are shown in Figure 6, parts b and d. The integral J_{SC} of the EQE curves of the devices are all in errors within 5% with the value from the J - V measurement. We note that the devices processed with MOB as the solvent exhibits higher V_{OC} than that of the corresponding device processed with CB. The reason is not clear yet and need further investigation.

Morphology. The effect of chemical structure and processing solvent on the morphology of the active layer in the PSC devices was investigated by transmission electron microscopy (TEM) and atomic force microscopy (AFM). The TEM results are shown in Figure 7. For PFDTOBT with alkyl side chains, more uniform phase separation morphology is observed when processed by CB compared to processed with MOB (Figure 7a,b). In contrast, for PFDTOBT-O2,

PFDTOBT-O3, and PFDTOBT-O4 with OEG side chains, more uniform and clear phase separation morphology is observed when processed by MOB compared to processed with CB (Figure 7c-h). The effect of processing solvent on the morphology of polymer:PC₆₁BM blend of the four polymers is in accordance with the corresponding PSC device performance. For the blend of PFDTOBT-O2:PC₆₁BM processed with MOB, which gives the best PSC device performance (Figure 7d), clear phase separation of donor polymer (relatively white region) and acceptor material (relative dark region) can be observed. However, the phase separation domain size is much larger than ideal (10–20 nm) for high photovoltaic performance.¹⁶ The AFM images are shown in Figure S2. For PFDTOBT with alkyl side chains, more uniform surface (root-mean-square (rms) roughness: 0.24 vs 0.32 nm) is observed when processed with CB compared to processed with MOB (Figure S2 a, e). In comparison, for PFDTOBT-O2 with OEG side chains, the film surface is more smooth when processed with MOB than that processed with CB.

Device Improvement. Although the device based on PFDTOBT-O2:PC₆₁BM processed with MOB exhibits the best photovoltaic performance, it still suffers from large phase separation domain size, which limits further device performance enhancement. To improve the morphology of the blend, we use 1,8-diiodooctane (DIO) as a solvent additive.¹⁷ We test the volume ratio (DIO/MOB) of 1 vol %, 3 vol %, 5 vol %, 7 vol % and 9 vol %, and find that 5 vol % is the optimized one (Figure S3 and Table S1, Supporting Information). As shown in the inset of Figure 8b, after adding 5 vol % DIO to MOB, the phase separation of PFDTOBT-O2:PC₆₁BM blend is more obvious and the phase separation domain size decreases to about 50 nm, which is beneficial for good photovoltaic performance. The resulting PSC device based on PFDTOBT-O2 processed with MOB and 5 vol % DIO shows the PCE of 4.04% with the V_{OC} of 1.03 V, J_{SC} of 7.54 mA/cm², and FF of 0.52 (Figure 8a and Table 3). The increased J_{SC} is confirmed by the EQE curve, which shows the average EQE value of about 55% (Figure 8b). The increase of J_{SC} and FF with DIO additive is due to the improved phase separation of the PFDTOBT-O2:PC₆₁BM active layer (the inset of Figure 8b). Considering the poor overlap of the absorption spectrum of PFDTOBT-O2 with solar spectra, we believe that a PCE of exceeding 4% is an exciting result for device of PFDTOBT-O2:PC₆₁BM. Indeed, this PCE value is among the highest reported for PSC devices of conjugated polymers with the same polymer backbone, poly(fluorene-*alt-co*-(4,7-di-2-thienyl-2,1,3-benzothiadiazole)).¹⁸ Our results indicate that OEG side chain is a successful strategy to make donor polymers suitable for processing with nonhalogenated solvent.

CONCLUSIONS

In summary, we have synthesized four conjugated polymers with oligo(ethylene glycol) (OEG) or alkyl chain as the side chain and investigated the effect of OEG side chain on the properties of conjugated polymers. Replacing alkyl chain with OEG chain can decrease the π - π stacking distance of polymer backbone in thin film from 0.44 to 0.41 nm despite of the length of OEG chain, because OEG chain is more flexible than alkyl chain. Compared with PFDTOBT with alkyl chain, PFDTOBT-O2 with OEG chain of similar length exhibits higher crystallinity, higher charge carrier mobility and narrower bandgap. As the length of OEG chain increasing, PFDTOBT-O3 and PFDTOBT-O4 exhibit decreased hole mobility due to the increased content of inert component in the polymers. The large polarity of OEG side chain makes the conjugated polymer suitable for PSC devices fabricated with polar nonhalogenated solvent. According to the new insight on conjugated polymers with OEG side chain, conjugated polymers with high charge carrier mobility by using OEG side chains with proper length may be anticipated.

ASSOCIATED CONTENT

Supporting Information

Synthesis procedure of the materials, characterization, fabrication of PSC devices and hole-only devices, absorption spectra of the materials in MOB solution, AFM topography images, J - V and EQE curves, and characteristics of the PSC devices. The Supporting Information is available free of charge on the ACS Publications website at DOI: 10.1021/acs.macromol.5b00702.

AUTHOR INFORMATION

Corresponding Authors

*(J.L.) E-mail: liujun@ciac.ac.cn.

*(L.W.) E-mail: lixiang@ciac.ac.cn.

Notes

The authors declare no competing financial interest.

ACKNOWLEDGMENTS

This work was financially supported by the 973 Project (No. 2014CB643504, 2015CB655001), the Nature Science Foundation of China (No. 51373165), the Strategic Priority Research Program of Chinese Academy of Sciences (No. XDB12010200), and the "Thousand Talents Program" of China.

REFERENCES

- (1) (a) Yu, G.; Gao, J.; Hummelen, J. C.; Wudl, F.; Heeger, A. J. *Science* **1995**, *270*, 1789. (b) Guo, X.; Baumgarten, M.; Müllen, K. *Prog. Polym. Sci.* **2013**, *38*, 1832. (c) Adachi, T.; Tong, L.; Kuwabara, J.; Kanbara, T.; Saeki, A.; Seki, S.; Yamamoto, Y. *J. Am. Chem. Soc.* **2013**, *135*, 870. (d) Dou, L. T.; Gao, J.; Richard, E.; You, J. B.; Chen, C. C.; Cha, K. C.; He, Y. J.; Li, G.; Yang, Y. *J. Am. Chem. Soc.* **2012**, *134*, 10071. (e) Zhang, L.; Colella, N. S.; Liu, F.; Trahan, S.; Baral, J. K.; Winter, H. H.; Mannsfeld, S. C. B.; Briseno, A. L. *J. Am. Chem. Soc.* **2013**, *135*, 844. (f) Liu, J.; Zhou, Q. G.; Cheng, Y. X.; Geng, Y. H.; Wang, L. X.; Ma, D. G.; Jing, X. B.; Wang, F. S. *Adv. Mater.* **2005**, *17*, 2974.
- (2) Gustafsson, G.; Cao, Y.; Treacy, G. M.; Klavetter, F.; Colaneri, N.; Heeger, A. J. *Nature* **1992**, *357*, 477.
- (3) (a) Li, W. S.; Yamamoto, Y.; Fukushima, T.; Saeki, A.; Seki, S.; Tagawa, S.; Masunaga, H.; Sasaki, S.; Takata, M.; Aida, T. *J. Am. Chem. Soc.* **2008**, *130*, 8886. (b) Zhang, X.; Chen, Z. J.; Wurthner, F. *J. Am. Chem. Soc.* **2007**, *129*, 4886. (c) Moon, J. H.; McDaniel, W.; MacLean, P.; Hancock, L. E. *Angew. Chem., Int. Ed.* **2007**, *46*, 8223.
- (4) (a) Kanimozhi, C.; Yaacobi-Gross, N.; Chou, K. W.; Amassian, A.; Anthopoulos, T. D.; Patil, S. *J. Am. Chem. Soc.* **2012**, *134*, 16532. (b) Shao, M.; He, Y. J.; Hong, K. L.; Rouleau, C. M.; Geohagan, D. B.; Xiao, K. *Polym. Chem.* **2013**, *4*, 5270. (c) Sax, S.; Rugen-Penkalla, N.; Neuhold, A.; Schuh, S.; Zojer, E.; List, E. J. W.; Mullen, K. *Adv. Mater.* **2010**, *22*, 2087. (d) Chang, W.-H.; Gao, J.; Dou, L. T.; Chen, C.-C.; Liu, Y. S.; Yang, Y. *Adv. Energy Mater.* **2014**, *4*, 1300864. (e) Chen, Y.; Zhang, S. Q.; Wu, Y.; Hou, J. H. *Adv. Mater.* **2014**, *26*, 2744.
- (5) (a) Zhou, H.; Yang, L.; Xiao, S.; Liu, S.; You, W. *Macromolecules* **2010**, *43*, 811. (b) Mei, J. G.; Bao, Z. N. *Chem. Mater.* **2014**, *26*, 604. (c) Lei, T.; Dou, J. H.; Pei, J. *Adv. Mater.* **2012**, *24*, 6457. (d) Mei, J. G.; Kim, D. H.; Ayzner, A. L.; Toney, M. F.; Bao, Z. A. *J. Am. Chem. Soc.* **2011**, *133*, 20130.
- (6) (a) Solmaz, T.; Fatemeh, J.; Ineke, V. S.; Catherine, K.; Satish, P.; Remco, W. A. H.; Ryan, C. C.; Laurence, L.; Dirk, J. M. V.; Thomas, J. C.; Jan, C. H.; L. Jan, A. K. *Adv. Funct. Mater.* **2015**, *25*, 150. (b) Sengwa, R. J. *Polym. Int.* **1998**, *45*, 43.
- (7) Boese, R.; Weiss, H. C.; Blaser, D. *Angew. Chem., Int. Ed.* **1999**, *38*, 988.
- (8) Yang, L. Q.; Zhou, H. X.; You, W. J. *Phys. Chem. C* **2010**, *114*, 16793.
- (9) (a) Du, C.; Li, C. H.; Li, W. W.; Chen, X.; Bo, Z. S.; Veit, C.; Ma, Z. F.; Wuerfel, U.; Zhu, H. F.; Hu, W. P.; Zhang, F. L. *Macromolecules* **2011**, *44*, 7617. (b) Svensson, M.; Zhang, F. L.; Veenstra, S. C.; Verhees, W. J. H.; Hummelen, J. C.; Kroon, J. M.; Ingnas, O.; Andersson, M. R. *Adv. Mater.* **2003**, *15*, 988. (c) Chen, M. H.; Hou, J.; Hong, Z.; Yang, G.; Sista, S.; Chen, L. M.; Yang, Y. *Adv. Mater.* **2009**, *21*, 4238.
- (10) (a) Liu, J.; Choi, H.; Kim, J. Y.; Bailey, C.; Durstock, M.; Dai, L. M. *Adv. Mater.* **2012**, *24*, 538. (b) Leclerc, M.; Ranger, M.; Belanger-Gariepy, F. *Acta Crystallogr. C* **1998**, *54*, 799.
- (11) Meng, B.; Fang, G.; Fu, Y. Y.; Xie, Z. Y.; Wang, L. X. *Nanotechnology* **2013**, *24*, 484004.
- (12) Qin, R. P.; Li, W. W.; Li, C. H.; Du, C.; Veit, C.; Schleiermacher, H. F.; Andersson, M.; Bo, Z. S.; Liu, Z. P.; Ingnas, O.; Wuerfel, U.; Zhang, F. L. *J. Am. Chem. Soc.* **2009**, *131*, 14612.
- (13) Wang, X. C.; Jiang, P.; Chen, Y.; Luo, H.; Zhang, Z. G.; Wang, H. Q.; Li, X. Y.; Yu, G.; Li, Y. F. *Macromolecules* **2013**, *46*, 4805.
- (14) (a) Thompson, B. C.; Frechet, J. M. J. *Angew. Chem., Int. Ed.* **2008**, *47*, 58. (b) Li, G.; Zhu, R.; Yang, Y. *Nat. Photonics* **2012**, *6*, 153. (c) Gunes, S.; Neugebauer, H.; Sariciftci, N. S. *Chem. Rev.* **2007**, *107*, 1324.
- (15) (a) Meng, B.; Fu, Y. Y.; Xie, Z. Y.; Liu, J.; Wang, L. X. *Polym. Chem.* **2015**, *6*, 805. (b) Duan, C. H.; Cai, W. Z.; Hsu, B. B. Y.; Zhong, C. M.; Zhang, K.; Liu, C. C.; Hu, Z. C.; Huang, F.; Bazan, G. C.; Heeger, A. J.; Cao, Y. *Energy Environ. Sci.* **2013**, *6*, 3022. (c) Chueh, C.-C.; Yao, K.; Yip, H.-L.; Chang, C.-Y.; Xu, Y.-X.; Chen, K.-S.; Li, C.-Z.; Liu, P.; Huang, F.; Chen, Y. W.; Chen, W.-C.; Jen, A. K.-Y. *Energy Environ. Sci.* **2013**, *6*, 3241. (d) Guo, X.; Zhang, M. J.; Cui, C. H.; Hou, J. H.; Li, Y. F. *ACS Appl. Mater. Interfaces* **2014**, *6*, 8190.
- (16) Brabec, C. J.; Heeney, M.; McCulloch, I.; Nelson, J. *Chem. Soc. Rev.* **2011**, *40*, 1185.
- (17) (a) Peet, J.; Kim, J. Y.; Coates, N. E.; Ma, W. L.; Moses, D.; Heeger, A. J.; Bazan, G. C. *Nat. Mater.* **2007**, *6*, 497. (b) Lou, S. J.; Szarko, J. M.; Xu, T.; Yu, L. P.; Marks, T. J.; Chen, L. X. *J. Am. Chem. Soc.* **2011**, *133*, 20661.
- (18) Slooff, L. H.; Veenstra, S. C.; Kroon, J. M.; Moet, D. J. D.; Sweelssen, J.; Koetse, M. M. *Appl. Phys. Lett.* **2007**, *90*, 143506.